Langmuir

Article

pubs.acs.org/Langmuir

Interpolymer Complexation: Comparisons of Bulk and Interfacial Structures

Beatrice Cattoz,[†,‡] Wiebe M. de Vos,[§,‡] Terence Cosgrove,[‡] Martin Crossman,[∥] Youssef Espidel,[‡] and Stuart W. Prescott*[,⊥,†]

[†]Department of Pharmaceutical, Chemical and Environmental Sciences, Faculty of Engineering and Science, University of Greenwich, Medway Campus, Central Avenue, Chatham Maritime, Kent ME4 4TB, U.K.

[‡]School of Chemistry, University of Bristol, Cantock's Close, Bristol BS8 1TS, U.K.

[§]Membrane Science and Technology, University of Twente, 7500 AE Enschede, The Netherlands

[∥]Port Sunlight Laboratory, Unilever Research, Quarry Road East, Bebington, The Wirral CH63 3JW, U.K.

[⊥]School of Chemical Engineering, UNSW Australia, UNSW Sydney, New South Wales 2052, Australia

Supporting Information

ABSTRACT: The interactions between the strong polyelectrolyte sodium poly(styrenesulfonate), NaPSS, and the neutral polymer poly(vinylpyrrolidone), PVP, were investigated in bulk and at the silica/solution interface using a combination of diffusion nuclear magnetic resonance spectroscopy (NMR), small-angle neutron scattering (SANS), solvent relaxation NMR, and ellipsometry. We show for the first time that complex formation occurs between NaPSS and PVP in solution; the complexes formed were shown not to be influenced by pH variation, whereas increasing the ionic strength increases the complexation of NaPSS but does not influence the PVP directly. The complexes formed contained a large proportion of NaPSS. Study of these interactions at the silica interface demonstrated that complexes also form at the nanoparticle interface where PVP is added in the system prior to NaPSS. For a constant PVP concentration and varying NaPSS concentration, the system remains stable until NaPSS is added in excess, which leads to depletion flocculation. Surface complex formation using the layer-by-layer technique was also reported at a planar silica interface.

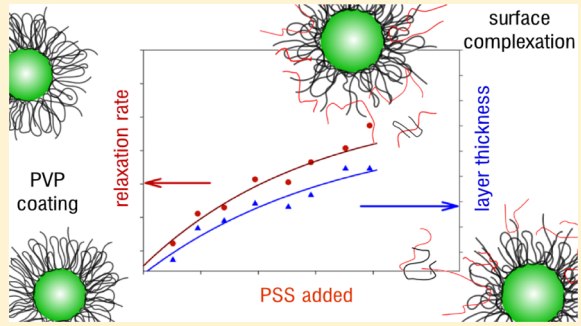

INTRODUCTION

The formation of interpolymer complexes in the bulk and the formation of polymer multilayers at the solid interface is a widely studied subject due to its potential industrial applications, from nanocoatings to drug release. Multilayer formation is often studied on flat surfaces, the layer-by-layer technique[1] being the preferred method for building mutlilayers. These interactions often occur through electrostatic interactions between polymers of opposite charge, and a considerable body of work has been published on the subject.[2−6] Shovsky et al.[6] investigated the bulk interactions between the strong polyelectrolyte sodium poly(styrenesulfonate), NaPSS, and bottle-brush copolymers composed of a cationic backbone and grafted nonionic segments. The effect of varying the density of nonionic segments on the complex structure was studied with static and dynamic light scattering and electrophoretic mobility. They found that increasing the density of the nonionic segments decreased the size of the complex. The mixing ratio of the polymer was also investigated, and it was found that larger aggregates were formed where NaPSS was present in excess but that the size remained similar between equimolar ratios and an excess of bottle-brush copolymers. They later investigated the same polymer pairs on silicon oxynitride surfaces;[7] adsorption was found to occur for cationic, neutral, and anionic complexes but the cationic complexes adsorbed in the largest amount.

The interactions between polymers, surfactants, and substrates are highly varied and have been widely studied; to understand the complicated phenomena that are manifest in these systems, a wealth of techniques have been employed including light scattering,[8] atomic force microscopy, AFM,[9,10] ellipsometry,[11] viscometry,[12] nuclear magnetic resonance spectroscopy, NMR,[13−15] neutron reflection,[16−18] and small-angle scattering.[14,19] The interactions responsible for multilayer formation have been studied theoretically and experimentally,[17,20] demonstrating that strong electrostatic attractions between oppositely charged polymers do not guarantee multilayer formation. Van der Waals and ionic interactions are also important factors in determining the ability to form multilayers.

The influence of the hydrophobicity of polymers on layer-by-layer assembly has been monitored with quartz crystal

Received: September 30, 2014
Revised: March 19, 2015
Published: March 20, 2015

DOI: 10.1021/la503870b
Langmuir 2015, 31, 4151−4159

microbalance, QCM, contact angle measurements, and AFM.[9,21] In these studies, a gold substrate was dipped repeatedly in high ionic strength poly(vinyl alcohol) solutions with a drying step between each dip. The polymer layer was shown to get thicker with increasing number of dips, demonstrating that the solvophobicity of the dried polymer can result in multilayer formation as well as polymer interactions.

Hydrogen bonding can also be responsible for interpolymer complexes and multilayer formation and has been widely studied.[11,13,22−27] A number of studies have investigated the interactions between poly(methacrylic acid), PMA, and poly(vinylpyrrolidone), PVP, a strong hydrogen receptor that forms strong bonds with acid derivative polymers. It was found that PVP forms multilayers with PMA up to a pH of 6.9.[26] Above this pH, multilayers do not form, due to the negative charge from ionization of the carboxylic acid functional group of the PMA and, hence, an electrostatic repulsion between the alternating polymer layers. Solid-state NMR was also used to determine the overall chain mobility between PMA and several hydrogen bond acceptors;[13] PVP was found to form a very strong bond with PMA.

Interpolymer complex formation between PVP and NaPSS has been previously reported in a viscometric study.[12] The phenomenon was only observed in a very specific experiment, and, in that work, the way of making the ternary solution had a significant effect indicating that these are kinetic structures. Mixing a stock solution of PVP with a stock solution of NaPSS showed no complex formation, while mixing pure NaPSS with a stock solution of PVP led to repulsive interactions. However, adding pure PVP to a NaPSS stock solution led to attractive interactions. The observed interactions were weak and presumed to originate from van der Waals forces rather than electrostatic or hydrogen bonding.

Here, we report on the interpolymer complex formation between NaPSS and PVP over a range of pH and ionic strengths. We additionally describe the formation of surface complexes at the silica nanoparticle interface and at the flat silica interface. Interpolymer complex formation is witnessed in solutions made from stock solution of both polymers. There is a substantial body of work documenting the adsorption of PVP onto silica;[19,28,29] however, the interactions between the like-charged NaPSS and silica are unfavorable toward adsorption. We believe it is also the first time surface complex formation (possibly including multilayer formation) has been observed at basic pH for a polymer pair composed of a strongly negatively charged polymer and a neutral, water-soluble homopolymer on a negatively charged interface. Bulk interactions between both polymers were investigated by diffusion NMR and small-angle neutron scattering (SANS). Solvent relaxation NMR and photocorrelation spectrscopy (PCS) are additionally used to determine that interactions occurring at the silica nanoparticle interface. Finally, ellipsometry allowed the measurement of the evolution of the overall polymer layer thickness following complex formation.

EXPERIMENTAL SECTION

Materials. The colloidal silica used was Bindzil 30/220 kindly provided by EKA Chemicals. It has an average particle diameter of 150 Å (equivalent to a surface area of 220 $m^2\ g^{-1}$). PVP ($\bar{M}_w$ = ca. 40 kg mol^{-1}; molecular mass dispersity (Đ) = 3.3) was obtained from Polysciences, NaPSS ($\bar{M}_n$ = 60.6 kg mol^{-1}; Đ = 1.04) was obtained from Polymer Source. Samples were prepared from stock solutions using Milli-Q water (or D_2O for SANS experiments). D_2O (99.94% D) was supplied by Goss Scientific. The samples for the interfacial study were prepared by weighing PVP stock solution, Bindzil 30/220, and solvent in a vial, and the mixtures were left to equilibrate on a roller-mixer for at least 12 h. The NaPSS was then added to the solution, and the sample was then left again on a roller-mixer for a further 48 h.

Pulsed Field Gradient Stimulated-Echo NMR. A Bruker DSX-400 MHz spectrometer using a Diff30 field gradient probe with 5 mm $^1H/^2H$ coil insert was used to obtain stimulated spin−echo pulsed field gradient (PFGSE-NMR)[30] measurements for each sample. This sequence produces an echo at time $(\tau_L + 2\tau)$, where τ is the time between the first and second radio frequency pulses (fixed at 6 ms for each sample) and τ_L is the time between the second and third radio frequency pulses. The gradient pulse duration, δ, was set to 1 ms, and the magnetic field gradient, G, was ramped from 0.05 to 10 T m^{-1}. The diffusion time, Δ, was set between 50 and 250 ms, depending on the sample. To maximize the signal-to-noise ratio, 64 scans were run over at least 50 gradient steps. The instrument was calibrated using a water/methanol reference sample. The stimulated-echo signals were Fourier-transformed, and the resulting decays (signal area as a function of the gradient strength) were fitted to

$$A(\tau_L + 2\tau) = A_0 \exp[-\gamma^2 G^2 \delta^2 (\Delta - \delta/3) D] \quad (1)$$

where A_0 is the initial peak area, A is the peak area for each gradient step, and γ is the gyromagnetic ratio of the nucleus, which is 2.675×10^8 rad T^{-1} s^{-1} for protons. The attenuation curves for any given sample are highly reproducible, and calculated uncertainties are smaller than the symbols so omitted from the plots. Equation 1 assumes Brownian motion to find the diffusion coefficients, D, for each chemically distinct species.

The average diffusion coefficients for the samples containing PVP were obtained by fitting the integrated peak area in the 1−4.2 ppm region while the average diffusion coefficients for NaPSS were obtained by fitting the integrated peak area in the 6−8 ppm region. The different polymers can be readily distinguished as shown in the characteristic one-dimensional (1D) NMR spectra of solutions of PVP, NaPSS, and a 1:1 mixture of PVP and NaPSS shown in the Supporting Information. Two-component fits were used to distinguish between complexed and uncomplexed polymer. Since the polymer chains fall into the slow exchange limit (if indeed there is any exchange of molecules between the complexed and uncomplexed states), the ratio of the intensities of the two diffusing components offering a direct measure of the relative number of monomer units contributing to that signal. The calculation provides uncertainties that are smaller than the symbols in the plotted data presented here.

Relaxation NMR. A Bruker MSL 300 MHz NMR spectrometer, using the CPMG pulse sequence, was used to obtain a relaxation decay curve for each sample. The time between the 180° pulses was 4 ms (i.e., τ = 2 ms), and the recycling delay was 13 s. At least 4096 echoes were collected in each scan, and the signal was averaged over four scans for each sample. The relaxation rate coefficient, $R_2 = 1/T_2$, for each relaxation decay curve, $M_y(t)$, was obtained by fitting each curve using a nonlinear least-squares algorithm to a first-order recovery:

$$M_y(t) = M_y(0)\, e^{-R_2 t} \quad (2)$$

where $M_y(0)$ is the transverse magnetization immediately after the 90° pulse and t represents the relaxation interval. The relaxation rate coefficient is presented as a specific relaxation rate enhancement:

$$R_{2sp} = \frac{R_2}{R_2^0} - 1 \quad (3)$$

where R_2^0 is the measured relaxation rate coefficient for an appropriate reference sample. In this work, the relaxation rate for the Bindzil dispersion was used for R_2^0, giving $R_{2sp} = 0$ for uncoated silica. Further details of this NMR technique are discussed extensively elsewhere.[31]

SANS. SANS experiments were performed on the D11 diffractometer at the high flux reactor of the Institut Laue-Langevin (ILL), Grenoble, France. D11 is a reactor-based diffractometer, and a neutron

DOI: 10.1021/la503870b
Langmuir 2015, 31, 4151−4159

wavelength of λ = 8 Å was employed at three different detector distances, D = 2.0, 8.0, 28.0 m. This setup corresponds to a Q range from 6.5 × 10^{-3} to 0.37 $Å^{-1}$. All spectra were normalized and corrected using the scattering of the empty cell. Scattering data were corrected for electronic noise and incoherent background using the scattering from a 1 mm H_2O sample corrected by the intensity scattered from the empty quartz cell.

The Beaucage model[32] was used to analyze the data presented in this study. It models the Guinier and Porod regions with a smooth transition between them and yields a radius of gyration and a Porod exponent. This model is able to reasonably approximate the scattering from many different types of particles, including fractal clusters, random coils, and ellipsoidal particles, etc. The empirical fit function is

$$I(Q) = G\exp\left(\frac{-(QR_g)^2}{3}\right) + \frac{C}{Q^d}\left[\mathrm{erf}\left(\frac{QR_g}{\sqrt{6}}\right)\right]^{3p} + I_{inc} \quad (4)$$

where G is the Guinier scaling factor, C is the Porod scaling factor, and p is the Porod exponent. The parameters used for fitting data to the Beaucage model are as follows: (1) power, p, the Porod exponent; (2) Porod scaling factor, C, in cm^{-1} sr^{-1}; (3) radius of gyration, R_g, of the polymer or particle in solution, measured in Å; (4) Guinier scaling factor, G, in cm^{-1} sr^{-1}; (5) incoherent background scattering, I_{inc}, for the sample, in cm^{-1}. Parameters 2 and 4 were not varied independently to avoid introducing undesired artifacts in the fitting procedure. Robust uncertainty analysis is therefore difficult, but the underlying trends in R_g and p are still evident.

PCS. The diffusion coefficients of the samples were measured using a Brookhaven Instruments Zeta Plus apparatus, fitted with a 15 mW laser (λ = 678 nm). The Stokes−Einstein equation was used to calculate the hydrodynamic diameter of the particles from the diffusion coefficient.

Viscosity. The viscosity of the bulk samples was measured with a BS/U/M miniature U-tube viscometer at 25 °C; three repeats of each measurement were performed. In order to account for the changes in viscosity of the samples induced by the increasing concentration of NaPSS in the PCS measurements, kinematic viscosity measurements were also performed on the samples.

Layer-by-Layer Deposition. A silicon wafer was first immersed in a solution containing 1.0 g L^{-1} PVP for 20 min and washed 3 times in Milli-Q water. The same wafer was then immersed in a solution containing 1.9 g L^{-1} NaPSS for 20 min and then washed 3 times in Milli-Q water. This procedure was repeated several times with the thickness of the polymer layer being characterized by ellipsometry between each polymer deposition step. Additionally, the thickness of the oxide layer on a silica wafer was measured by ellipsometry prior to the experiment.

Ellipsometry. Ellipsometry measurements were performed using a variable-angle spectroscopic instrument (J. A. Woollam Co. Inc., Lincoln, NE, USA) with a rotating analyzer configuration. The chosen wavelength, λ, ranged from 400 to 800 nm. Measurements were performed with the incident light beam set at 72° with respect to the sample normal. The refractive indexes used to fit the data were as follows: silicon, 3.85; silica, 1.46; PVP, 1.51;[33] NaPSS, 1.48.[34] The ellipsometry spectra of the silicon oxide layer, the PVP layer, and the NaPSS layer were obtained via successive measurements; the thickness of each of the layers was thus obtained independently.

RESULTS AND DISCUSSION

Bulk Interactions. Pulsed field gradient NMR was used to measure the diffusion coefficients of solutions containing 5 wt % polymer or mixture of polymers in D_2O. Figure 1 shows the attenuation curves of the peak intensities of the single polymer samples and the samples containing a 1:1 mixture of both polymers in pure solvent (for both PVP and NaPSS related peaks). The effect of salt concentration was also investigated, and the plots of the related attenuation curves can be found in the Supporting Information.

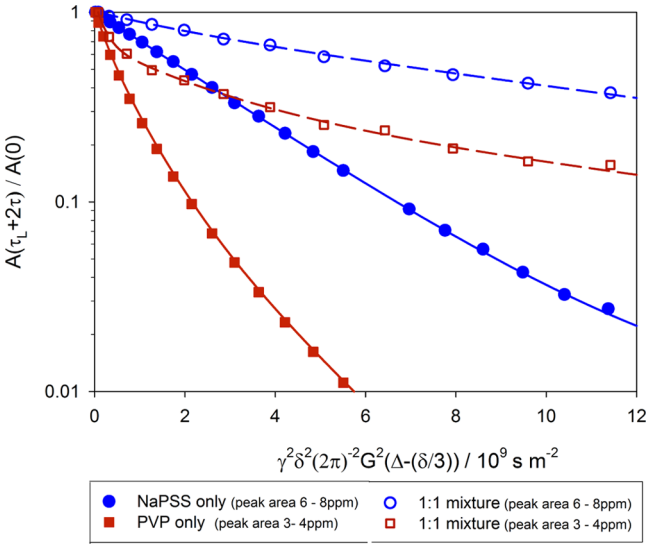

Figure 1. Attenuation curves of PVP, NaPSS, and a mixture of PVP and NaPSS with a total of 5 wt % polymer in each case. Solid lines are fits to a two-component diffusion function.

The attenuation function has a steeper slope for PVP than for NaPSS indicating a faster diffusion coefficient. This is not surprising as PVP is expected to adopt a random coil configuration and hence is more compact than NaPSS, which, due to its charge, is assumed to be in a more rigid and extended configuration.[35] The slopes of the attenuation function for the sample containing the mixture of polymers are much shallower than the slopes from the related individual polymer. This indicates that polymer interaction is occurring, although these slopes being dissimilar reveal that only a portion of the polymers are interacting. If every polymer chain was involved in the complexation, they would all diffuse at the same speed; hence, the slopes of the attenuation function for PVP and NaPSS would be identical. The averaged diffusion coefficients, D_A, calculated from fitting the attenuation plots (Figure 1) with eq 1, are recorded in Table 1.

Table 1. Diffusion Coefficients, Viscosities, and Hydrodynamic Radii from Individual Polymer Solutions

polymer[a]	solvent medium	$D_A/(10^{11}$ m^2 $s^{-1})$	viscosity/cSt	R_H[b]/Å
PVP	0 mM NaCl	4.62	2.41	47
	15 mM NaCl	4.63	2.45	47
	1 M NaCl	4.62	2.60	47
NaPSS	0 mM Nacl	0.90	5.94	242
	15 mM NaCl	1.03	5.24	212
	1 M NaCl	2.44	2.25	89

[a]Total polymer concentration fixed at 5 wt % for all experiments. [b]Viscosity of the pure solvent was used for the calculation.

The NaPSS in solution could be described by a single diffusion coefficient, which is expected for a low dispersity polymer in solution below its overlap concentration.[36] PVP, however, could not be modeled by a single-component diffusion, and this is due to the high polydispersity of the polymer;[37] data treatment used a three-component diffusion model to fit these nonideal cases. For the samples where the diffusion coefficient results contained more than one component, the weight-average diffusion coefficient, D_A, was calculated. The hydrodynamic radii of the polymers were

DOI: 10.1021/la503870b
Langmuir 2015, 31, 4151−4159

Table 2. Diffusion Coefficients and Viscosities of Mixed Polymer Solution[a]

		0 mM NaCl	15 mM NaCl	1 M NaCl
6−8 ppm peak area (NaPSS)	$D_1/(10^{11}\ m^2\ s^{-1})$	0.18	0.17	0.53
	component/%	80	94	100
	$D_2/(10^{11}\ m^2\ s^{-1})$	0.90	1.03	2.44
	component/%	20	6	0
3−4 ppm peak area (PVP)	$D_1/(10^{11}\ m^2\ s^{-1})$	0.18	0.17	0.53
	component/%	28	26	21
	$D_{A(2,3)}$[b]$/(10^{11}\ m^2\ s^{-1})$	6.9	5.18	6.94
	component/%	72	74	79
% polymer complexed		54	60	61
NaPSS:PVP ratio in complex[c]		60:40	66:34	71:29
sample viscosity/(cSt ± 0.1)		24.5	17.5	5.2

[a]Total polymer concentration fixed at 5 wt % for all experiments. [b]Weighted average of the fast diffusing components D_2 and D_3. [c]Ratio of number of monomer units in the complex, calculated by scaling the percentage of each D_1 component by their respective monomer molar mass (111 g/mol for PVP monomer and 206 g/mol for NaPSS monomer).

calculated from the diffusion coefficients using the Stokes−Einstein equation. The PVP chains were not affected by the change in ionic strength, whereas the NaPSS chains where shown to become more compact upon addition of salt.[35]

The resulting diffusion coefficients and viscosities for the samples containing both polymers are shown in Table 2. The diffusion coefficients for the peak area related to NaPSS were best described by two distinct diffusion coefficients, D_2 being the same value as the single polymer in solution and reported in Table 1. The slower component, D_1, then corresponds to the diffusion of NaPSS interacting with PVP; the NaPSS diffuses more slowly because it has formed a larger object than the single polymer.

The hydrodynamic radii of the complexes could not be determined by the Stokes−Einstein equation because the viscosity of the solvent is influenced by the presence of the noninteracting polymers, and the viscosity of only these free polymers in the system could not be determined. The peak area corresponding to PVP in the mixed system was also fitted to three diffusion coefficients: D_1 corresponds to the diffusion of the interacting polymers while the two other diffusion coefficients correspond to the noninteracting chains and are reported in Table 2 as a weight-average D_A (in the same manner as in Table 1). The average diffusion coefficient of uncomplexed PVP reported in Table 2 is slightly faster than in the PVP-only experiments reported in Table 1. PVP has a large molecular mass dispersity (Đ = 3.3, according to supplier specifications), so it has a wide range of chain lengths. Interpolymer complexes are favored by longer chain lengths,[8,38,39] so it is then plausible that, in the present case, the larger chains of PVP interact preferentially with NaPSS. The $\bar{M}_w$ of the PVP remaining free in solution is then expected to be less than 40 kDa, and thus the chains would on average be smaller and diffuse at a faster rate.

The weighted percentage of the number of polymer chains found for each diffusion coefficient gives a measure of the percentage of polymer involved in the complexation (see Table 2 and Figure 2). These data show that most of the NaPSS chains are part of the complexes and that increasing the salt concentration increases the percentage of NaPSS complexed; at 1 M NaCl every NaPSS chain is part of a complex. On the other hand, only about a quarter of the PVP chains are involved in complexes and increasing the salt concentration seems to slightly decrease the percentage of PVP involved in the complexes.

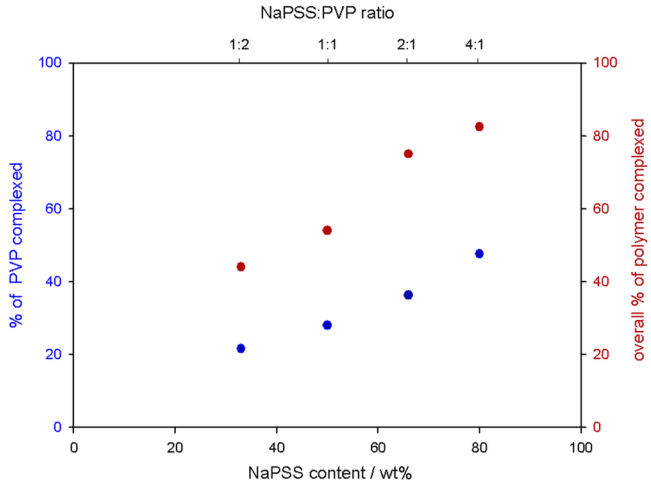

Figure 2. Percentage of PVP and overall polymer complexed against NaPSS:PVP ratio.

These samples are then composed of about half of NaPSS-rich interpolymer complexes, some free PVP, and a small amount of free NaPSS. Salt addition leads to polymer complexes with more NaPSS although the overall amount of polymer complexed increases only slightly; in the case of 1 M NaCl, all the NaPSS is involved in the complexation and only PVP remains free in solution. The ratio of monomer in the complexes was also calculated and is recorded in Table 2; this also shows that the complexes formed with these polymers are not stoichiometric.

The viscosity of these solutions was also measured. The viscosity for the mixture of samples without added salt is very high, suggesting some polymer bridging between complexes. The viscosity decreases with increasing salt concentration, implying that more compact interpolymer complexes are formed. These trends were also observed for the samples containing NaPSS alone, indicating that the ionic strength affects the configuration of the complexes in a fashion similar to that of NaPSS alone.

These results establish that interparticle interactions are occurring between PVP and NaPSS in solutions where mixtures are made of polymer stock solutions. These results differ from the findings of the previous viscometric study from García et al.,[12] where interactions were witnessed only in samples in which pure PVP was mixed with NaPSS solution. The main

DOI: 10.1021/la503870b
Langmuir 2015, 31, 4151−4159

difference in our experiment is the polymer concentration of the solutions; their study was performed on solutions 50 times less concentrated than the present study.

In order to investigate the effect of polymer mixing ratio, ionic strength, and pH on the formation of the complexes, SANS measurements were performed. In these experiments, the overall polymer concentration was kept constant at 5 wt %. Figure 3 shows the scattering from individual polymers and the

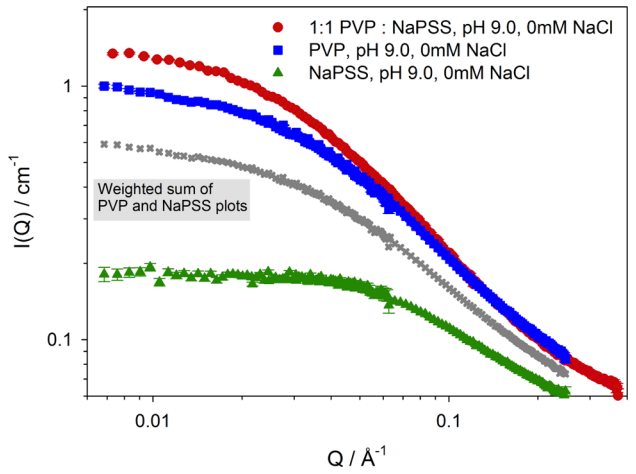

Figure 3. SANS from 5 wt % PVP, NaPSS, and a 1:1 mixture of PVP and NaPSS. Calculated data for a noninteracting mixture of PVP and NaPSS also shown for comparison, showing that the two polymers are interacting in solution.

1:1 mixture of polymers; each solution contained 5 wt % polymer, and the solvent was adjusted to pH 9. The scattering intensity of the mixture of polymers is higher than individual polymers, again clearly showing that interpolymer interactions are occurring. In the absence of interactions, the scattering of the mixture should resemble the weighted sum of the scattering plots from the individual polymers.

The effect of ionic strength on the scattering of 1:1 mixtures at pH 9 is shown in Figure 4. The scattering from these samples is very similar in the high Q region ($Q > 0.04$ Å^{-1}), but in the

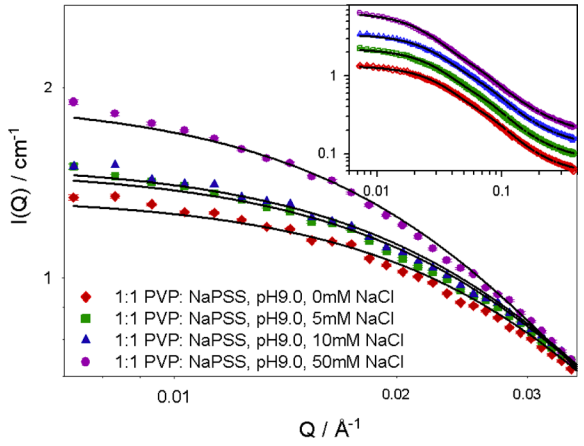

Figure 4. SANS from PVP and NaPSS mixtures. The total amount of polymer is 5 wt % in each case with varying salt concentrations. Main plot focuses on low Q data where differences in scattering are observed. Insert represents the full Q range; data are shifted vertically for clarity. For both graphs, solid lines are fits using the Beaucage model.

low Q region, the scattering intensity increases with increasing salt concentration. This can be attributed to the formation of either larger aggregates or more numerous aggregates. The SANS data were analyzed with the Beaucage model;[32] an example of the fits obtained is shown in Figure 4. Fitting the data using this model yields information on the overall radius of gyration of the polymers and complexes in solution and the power law regime of the mixtures. Fitting these samples to one R_g is not an ideal representation of the system as we have found from the diffusion NMR study that, in the case of the 1:1 polymer mixture, not all polymer chains take part in the interpolymer complexes and some chains do remain free in solution. However, because the complexes formed are larger than individual polymer chains, they are expected to dominate the scattering. It was found in the NMR study that most of the NaPSS was involved in interpolymer complexes and that the chains that were free in solution were mostly PVP chains. It is then assumed that the scattering observed in these polymer mixtures arises mainly from the complexes and to a lesser extent from the free PVP chains. Furthermore, the configuration of PVP chains is not influenced by pH or ionic strength variations; hence the trends observed in the mixtures with these variations should not be influenced by the presence of the free polymer.

The radii of gyration and the mass fractal dimensions extracted from the fitting are plotted in Figure 5. Figure 5a shows the fractal dimension plotted against the ratio of polymer in the system (overall concentration = 5.0 wt %); all of the samples are fitted to an average mass fractal dimension between 1.5 and 2.0. This relates to aggregate structures ranging from a fully swollen coil (fractal dimension = 1.5) to a Gaussian chain in a dilute solution (fractal dimension = 2.0), while a branched polymer would have a slightly higher fractal dimension;[40] the fractal dimension of PVP only in solution is 2.0.[41] The mass fractal dimension, F_D, decreases as the ratio of NaPSS in the system increases; this trend is observed through the whole data set (pH and ionic strength variation). It was determined by diffusion NMR that, in a 1:1 mixture, most of the NaPSS is involved in the interpolymer complex, whereas about a quarter of the PVP is complexed. Increasing the ratio of NaPSS is thus expected to lead to an increase in the concentration of the interpolymer complex.

The decrease in fractal dimension observed with increasing NaPSS ratio suggests that the complexes are in a less compact configuration than the free PVP. This trend is explained by the rod-like configuration of NaPSS at low ionic strength.[35] The mass fractal dimension was shown to decrease with increasing salt concentration as shown in Figure 5. Taken in conjunction with the increasing R_g, this would indicate that less dense and larger aggregates are being formed, presumably also from a larger number of polymer chains; F_D and R_g can vary independently once the aggregation number is allowed to vary.[42] We note that there are potential limitations in the measurement of the fractal dimension using the Beaucage model[43] and restrict our subsequent analysis to the radius of gyration data.

The overall radius of gyration was shown to decrease with increasing PVP:NaPSS ratio, as seen in Figure 5b. This may be explained by the increasing concentration of free PVP chains in solution (as shown in Figure 2), which would thus have a larger effect on the overall R_g measured here. The variation in pH leads to only small changes in the complex size (see the Supporting Information), and no trend is identified over this

DOI: 10.1021/la503870b
Langmuir 2015, 31, 4151−4159

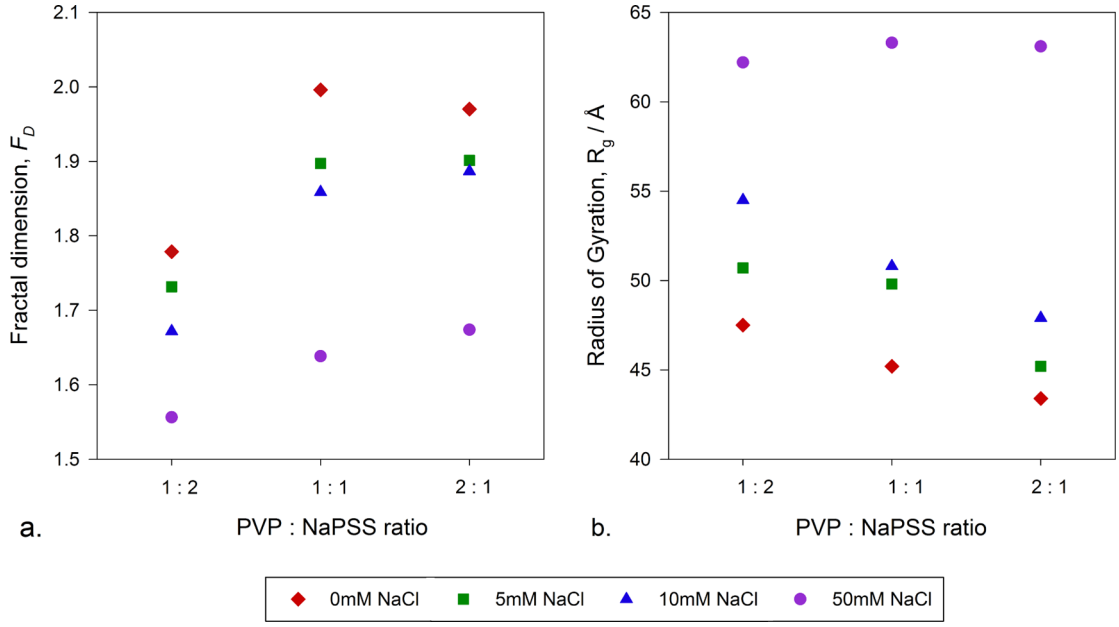

Figure 5. Radii of gyration and mass fractal dimensions of mixtures of PVP and NaPSS at pH 9; data extracted from fits with Beaucage model.

data set. This is consistent with the findings from the mass fractal dimension. The ionic strength has a noticeable effect on the radius of gyration of the complexes: increasing the ionic strength leads to an increase in the overall R_g, and this trend is present throughout the entire data set.

The scattering from the aggregates was expected to dominate, leading to a large increase in the scattering intensity and in the mass fractal dimension. The intensity enhancement, although observed in this data set, is fairly small, suggesting that the complexes do not form large compact individual aggregates but probably adopt a more network-like structure with polymer coils interacting but retaining some of their shape and individuality.

The effect of pH was also investigated, and the same SANS experiments were also performed at pH 7 and 3.5. The SANS data were analyzed using the same model; the results of fitting showed that there is no variation in size or fractal dimension with pH (see the Supporting Information).

Interfacial Interactions. While PVP adsorbs onto silica nanoparticles,[19,28,29] NaPSS does not adsorb onto silica and depletion induced attraction occurs in such systems;[44] it is then interesting to investigate what interactions would dominate in a system composed of silica, PVP, and NaPSS. We first look at interactions at the nanoparticle interface and then describe interactions on flat silica surfaces.

NaPSS complexation with PVP preadsorbed onto silica was measured using a combination of solvent relaxation NMR and PCS. Samples were made with a constant Bindzil 30/220 concentration of 2.5 wt % and constant PVP concentration of $[PVP]_{added}$ = 1. 0 mg m^{-2} (silica unit area); this concentration was previously shown to give near-full surface coverage.[19,31,45] The NaPSS amounts ranged from $[NaPSS]_{added}$ = 0.5 to 5.0 mg m^{-2} (silica unit area). These samples were used for the solvent relaxation NMR investigation and then diluted by a factor of ~4 prior to PCS measurements. Solvent relaxation measurements were also performed on aqueous solutions of PVP, NaPSS, and mixtures of PVP and NaPSS to confirm that this has minimal effect on R_2.

Figure 6 shows both solvent relaxation NMR and PCS for the adsorption of NaPSS onto PVP preadsorbed onto silica

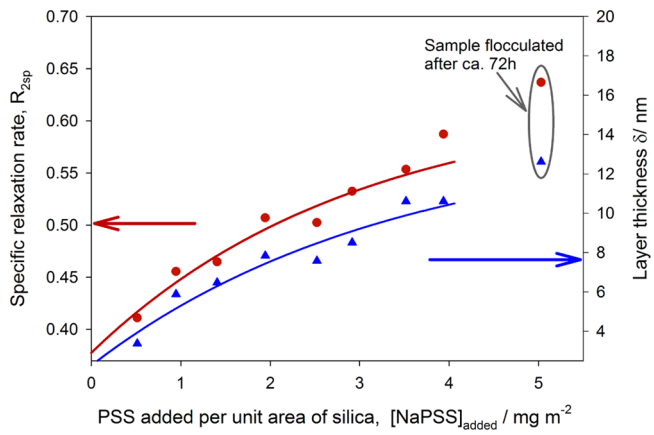

Figure 6. Adsorbed NaPSS on PVP preadsorbed on silica particles measured by solvent relaxation NMR (circles, left axis) and PCS (triangles, right axis). PVP added at 1.0 mg m^{-2} based on the silica surface area. Lines are a guide to the eye; the repeatability of the measurements is approximately 5%.

nanoparticles. The relaxation rate R_{2sp} is enhanced by addition of NaPSS indicating an increase in the near-surface polymer concentration in contrast to stripping the preadsorbed polymer as has been previously observed in other complexation studies;[19,46] removal of the PVP from the surface would give a reduction of R_{2sp} as we have previously described.[19] The resistance of the PVP to stripping is consistent with previous reports that PVP adsorbs to silica more strongly than PEO.[15,45] The layer thickness measured by PCS also increased upon NaPSS addition, confirming that more polymer adsorbs to the silica nanoparticle.

The sample containing $[NaPSS]_{added}$ = 5.0 mg m^{-2} was unstable and flocculated shortly after it was measured. Although the near-surface coverage is reached at $[PVP]_{added}$ = 1. 0 mg m^{-2}, the actual adsorbed amount of PVP was $[PVP]_{ads}$ ~ 0.5

DOI: 10.1021/la503870b
Langmuir 2015, 31, 4151−4159

mg m^{-2} as measured by SANS[19] and UV−vis spectrophotometry (see the Supporting Information). These samples therefore contain some PVP free in solution allowing for NaPSS to complex with both the free and adsorbed PVP and adsorb onto the PVP layer. The study of these mixtures of polymers in bulk by diffusion NMR (Table 2) revealed that the complexes formed are NaPSS-rich and contain 4−5 times more NaPSS than PVP. This would explain why the R_{2sp} and layer thickness keep increasing up to such a high polymer concentration.

The sample containing the highest concentration of NaPSS flocculated, and it may be hypothesized that, at this point, all of the PVP in the system was involved with NaPSS in making interpolymer surface complexes. Adding more polyelectrolyte is then equivalent to adding a nonadsorbing polymer to the system, which destabilizes the system and leads to depletion flocculation.

Ellipsometry was then used to determine if multilayer formation could occur with these polymers by using the layer-by-layer technique. PVP and NaPSS layers were alternately deposited on a silicon wafer, and, between each polymer addition step, the thickness of the total polymer layer was measured. The evolution of the polymer layer thickness with increasing number of polymer layers is shown in Figure 7. This

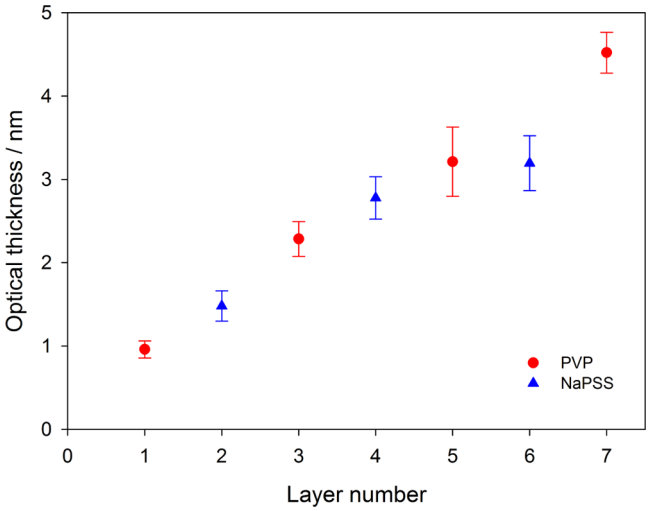

Figure 7. Ellipsometry measurement of the thickness of polymer layers adsorbed onto a silica wafer. Uncertainties are the standard deviation from multiple repeat measurements.

figure clearly shows the increase in layer thickness as PVP and NaPSS layers are deposited alternatively onto silica wafers, confirming the complexation of PVP with NaPSS, either in the form of uniform multilayers or of a more patchy conformation.

Multilayer formation using the layer-by-layer technique first reported by Decher and Hong[1] has been widely used. Multilayer formation is usually driven by electrostatic interactions between a polyanion and a polycation or by hydrogen-bonding interactions between a polyelectrolyte in its nonionized form and a nonionic polymer. In this system such interactions are not present, and a different intermolecular force must be involved to give the observed increase in polymer layer thickness. Although it is not clear what types of interactions are occurring between these two polymers, it is plausible that the sulfonate groups from NaPSS interact with the nitrogen groups from PVP; NaPSS has been shown to interact with polyaniline with such a mechanism.[47−49] PVP is also known to have a strong binding affinity with aromatic compounds,[50−52] so the interaction exhibited in this system may also arise from π-interactions between PVP and NaPSS which have previously been shown to be sufficient to lead to polymer adsorption.[10] The experiment presented here shows that this attraction is quite important since one would expect the negatively charged NaPSS layers to strongly repel each other, but clearly the attractive interaction is large enough to overcome this. It is reasonable to postulate that this interaction is also a significant contributor to the formation of the bulk complexes characterized here with NMR and SANS.

CONCLUSION

The interactions between neutral polymer PVP and the strong polyelectrolyte NaPSS have been studied both in bulk and at the silica interface. We show for the first time, using diffusion NMR, that PVP and NaPSS interpolymer complexes form in solution and that these complexes were NaPSS-rich. An increase in ionic strength favors the complexation of NaPSS but has no direct effect on PVP. It was also proposed that the larger molecular weight fractions (larger contour length) of PVP chains interact preferentially with NaPSS. SANS revealed that the complex formation was not influenced by pH (within the range studied) and that increasing ionic strength led to formation of larger complexes.

The interactions between PVP and NaPSS at the silica interface were studied at pH 9. Using a combination of solvent relaxation NMR and PCS, it was shown that complex formation at the silica nanoparticle interface occurs. Adding NaPSS to a system containing silica with PVP both adsorbed at the interface and free in solution leads to an increase in polymer concentration near the interface and an increase in thickness of the adsorbed layer. This system was found to be stable up to a 5:1 ratio of NaPSS to PVP, beyond which flocculation was observed. It is believed that once NaPSS is in excess and there is no free PVP to form complexes with it, the NaPSS then becomes a nonadsorbing polymer and leads to depletion flocculation. There are also indications of multilayer or complex formation on a silicon wafer, using the layer-by-layer technique as measured by ellipsometry.

ASSOCIATED CONTENT

Supporting Information

Figures showing 1D NMR data, additional PFGSE NMR diffusion data, and further SANS data. This material is available free of charge via the Internet at http://pubs.acs.org.

AUTHOR INFORMATION

Corresponding Author

*E-mail: s.prescott@unsw.edu.au.

Notes

The authors declare no competing financial interest.

ACKNOWLEDGMENTS

We are grateful to the EPSRC and Unilever for funding and the Institut Laue-Langevin (ILL) for neutron beam time (Proposal 9-12-251). Dr. Isabelle Grillo (ILL) is thanked for her excellent support during the SANS experiments.

DOI: 10.1021/la503870b
Langmuir 2015, 31, 4151−4159

REFERENCES

(1) Decher, G.; Hong, J.-D. Buildup of ultrathin multilayer films by a self-assembly process, 1 consecutive adsorption of anionic and cationic bipolar amphiphiles on charged surfaces. *Makromol. Chem., Macromol. Symp.* **1991**, *46*, 321−327.

(2) Schlenoff, J. B. Retrospective on the Future of Polyelectrolyte Multilayers. *Langmuir* **2009**, *25*, 14007−14010.

(3) de Villiers, M. M.; Otto, D. P.; Strydom, S. J.; Lvov, Y. M. Introduction to nanocoatings produced by layer-by-layer (LbL) self-assembly. *Adv. Drug Delivery Rev.* **2011**, *63*, 701−715.

(4) Lavalle, P.; Voegel, J.-C.; Vautier, D.; Senger, B.; Schaaf, P.; Ball, V. Dynamic Aspects of Films Prepared by a Sequential Deposition of Species: Perspectives for Smart and Responsive Materials. *Adv. Mater.* **2011**, *23*, 1191−1221.

(5) Han, L.; Mao, Z.; Wuliyasu, H.; Wu, J.; Gong, X.; Yang, Y.; Gao, C. Modulating the Structure and Properties of Poly(sodium 4-styrenesulfonate)/Poly(diallyldimethylammonium chloride) Multilayers with Concentrated Salt Solutions. *Langmuir* **2012**, *28*, 193−199.

(6) Shovsky, A.; Varga, I.; Makuska, R.; Claesson, P. M. Formation and Stability of Water-Soluble, Molecular Polyelectrolyte Complexes: Effects of Charge Density, Mixing Ratio, and Polyelectrolyte Concentration. *Langmuir* **2009**, *25*, 6113−6121.

(7) Shovsky, A.; Bijelic, G.; Varga, I.; Makuska, R.; Claesson, P. M. Adsorption Characteristics of Stoichiometric and Nonstoichiometric Molecular Polyelectrolyte Complexes on Silicon Oxynitride Surfaces. *Langmuir* **2011**, *27*, 1044−1050.

(8) Tsuchida, E.; Osada, Y.; Ohno, H. Formation of interpolymer complexes. *J. Macromol. Sci., Phys.* **1980**, *17*, 683−714.

(9) Serizawa, T.; Hashiguchi, S.; Akashi, M. Stepwise Assembly of Ultrathin Poly(vinyl alcohol) Films on a Gold Substrate by Repetitive Adsorption/Drying Processes. *Langmuir* **1999**, *15*, 5363−5368.

(10) Prescott, S. W.; Fellows, C. M.; Considine, R. F.; Drummond, C. J.; Gilbert, R. G. The interactions of amphiphilic latexes with surfaces: The effect of surface modifications and ionic strength. *Polymer* **2002**, *43*, 3191−3198.

(11) Stockton, W. B.; Rubner, M. F. Molecular-Level Processing of Conjugated Polymers. 4. Layer-by-Layer Manipulation of Polyaniline via Hydrogen-Bonding Interactions. *Macromolecules* **1997**, *30*, 2717−2725.

(12) García, R.; Gómez, C. M.; Porcar, I.; Figueruelo, J. E.; Campos, A. Viscometric study of mixtures of neutral and charged polymers in aqueous solution. *Eur. Polym. J.* **1997**, *33*, 1723−1730.

(13) Fortier-McGill, B.; Toader, V.; Reven, L. Chain Dynamics of Water-Saturated Hydrogen-Bonded Polymer Complexes and Multilayers. *Macromolecules* **2011**, *44*, 2755−2765.

(14) Cattoz, B.; de Vos, W. M.; Cosgrove, T.; Crossman, M.; Prescott, S. W. Manipulating Interfacial Polymer Structures through Mixed Surfactant Adsorption and Complexation. *Langmuir* **2012**, DOI: 10.1021/la300282m.

(15) Cooper, C. L.; Cosgrove, T.; van Duijneveldt, J. S.; Murray, M.; Prescott, S. W. Competition between polymers for adsorption on silica: A solvent relaxation NMR and small-angle neutron scattering study. *Langmuir* **2013**, *29*, 12670−12678.

(16) Singh, S.; Junghans, A.; Waltman, M. J.; Nagy, A.; Iyer, R.; Majewski, J. Neutron reflectometry characterization of PEI-PSS polyelectrolyte multilayers for cell culture. *Soft Matter* **2012**, *8*, 11484−11491.

(17) de Vos, W. M.; Mears, L. L. E.; Richardson, R. M.; Cosgrove, T.; Barker, R.; Prescott, S. W. Non-uniform hydration and odd-even effects in polyelectrolyte multilayers under a confining pressure. *Macromolecules* **2013**, *46*, 1027−1034.

(18) Abbott, S. B.; de Vos, W. M.; Mears, L. L. E.; Cattoz, B.; Skoda, M. W. A.; Barker, R.; Richardson, R. M.; Prescott, S. W. Is Osmotic Pressure Relevant in the Mechanical Confinement of a Polymer Brush. *Macromolecules* **2015**, DOI: 10.1021/ma502246r.

(19) Cattoz, B.; Cosgrove, T.; Crossman, M.; Prescott, S. W. Surfactant-Mediated Desorption of Polymer from the Nanoparticle Interface. *Langmuir* **2012**, *28*, 2485−2492.

(20) Kotov, N. A. Layer-by-layer self-assembly: The contribution of hydrophobic interactions. *Nanostruct. Mater.* **1999**, *12*, 789−796.

(21) Serizawa, T.; Kamimura, S.; Kawanishi, N.; Akashi, M. Layer-by-Layer Assembly of Poly(vinyl alcohol) and Hydrophobic Polymers Based on Their Physical Adsorption on Surfaces. *Langmuir* **2002**, *18*, 8381−8385.

(22) Such, G. K.; Johnston, A. P. R.; Caruso, F. Engineered hydrogen-bonded polymer multilayers: From assembly to biomedical applications. *Chem. Soc. Rev.* **2011**, *40*, 19−29.

(23) Kharlampieva, E.; Kozlovskaya, V.; Sukhishvili, S. A. Layer-by-Layer Hydrogen-Bonded Polymer Films: From Fundamentals to Applications. *Adv. Mater.* **2009**, *21*, 3053−3065.

(24) Kozlovskaya, V.; Yakovlev, S.; Libera, M.; Sukhishvili, S. A. Surface Priming and the Self-Assembly of Hydrogen-Bonded Multilayer Capsules and Films. *Macromolecules* **2005**, *38*, 4828−4836.

(25) Zhunuspayev, D. E.; Mun, G. A.; Hole, P.; Khutoryanskiy, V. V. Solvent Effects on the Formation of Nanoparticles and Multilayered Coatings Based on Hydrogen-Bonded Interpolymer Complexes of Poly(acrylic acid) with Homo- and Copolymers of *N*-Vinyl Pyrrolidone. *Langmuir* **2008**, *24*, 13742−13747.

(26) Sukhishvili, S. A.; Granick, S. Layered, Erasable, Ultrathin Polymer Films. *J. Am. Chem. Soc.* **2000**, *122*, 9550−9551.

(27) Erel-Unal, I.; Sukhishvili, S. A. Hydrogen-Bonded Multilayers of a Neutral Polymer and a Polyphenol. *Macromolecules* **2008**, *41*, 3962−3970.

(28) Cohen Stuart, M. A.; Mulder, J. Adsorbed polymers in aqueous media the relation between zeta potential, layer thickness and ionic strength. *Colloids Surf.* **1985**, *15*, 49−55.

(29) Cooper, C. L.; Cosgrove, T.; van Duijneveldt, J. S.; Murray, M. W.; Prescott, S. W. Colloidal particles in competition for stabilizer: A solvent relaxation NMR study of polymer adsorption and desorption. *Langmuir* **2012**, *28*, 16588−16595.

(30) Tanner, J. E. Use of the Stimulated Echo in NMR Diffusion Studies. *J. Chem. Phys.* **1970**, *52*, 2523−2526.

(31) Cooper, C. L.; Cosgrove, T.; van Duijneveldt, J. S.; Murray, M.; Prescott, S. W. The Use of Solvent Relaxation NMR to Study Colloidal Suspensions. *Soft Matter* **2013**, *9*, 7211−7228.

(32) Beaucage, G. Approximations Leading to a Unified Exponential/Power-Law Approach to Small-Angle Scattering. *J. Appl. Crystallogr.* **1995**, *28*, 717−728.

(33) Slistan-Grijalva, A.; Herrera-Urbina, R.; Rivas-Silva, J.; Avalos-Borja, M.; Castillon-Barraza, F.; Posada-Amarillas, A. Classical theoretical characterization of the surface plasmon absorption band for silver spherical nanoparticles suspended in water and ethylene glycol. *Phys. E (Amsterdam, Neth.)* **2005**, *27*, 104−112.

(34) Ruths, J.; Essler, F.; Decher, G.; Riegler, H.; Polyelectrolytes, I. Polyanion/Polycation Multilayers at the Air/Monolayer/Water Interface as Elements for Quantitative Polymer Adsorption Studies and Preparation of Hetero-superlattices on Solid Surfaces. *Langmuir* **2000**, *16*, 8871−8878.

(35) Adamczyk, Z.; Jachimska, B.; Jasinski, T.; Warszynski, P.; Wasilewska, M. Structure of poly (sodium 4-styrenesulfonate) (PSS) in electrolyte solutions: Theoretical modeling and measurements. *Colloids Surf., A* **2009**, *343*, 96−103.

(36) Masaro, L.; Zhu, X. Physical models of diffusion for polymer solutions, gels and solids. *Prog. Polym. Sci.* **1999**, *24*, 731−775.

(37) Callaghan, P. T.; Pinder, D. N. Influence of polydispersity on polymer self-diffusion measurements by pulsed field gradient nuclear magnetic resonance. *Macromolecules* **1985**, *18*, 373−379.

(38) Khutoryanskiy, V.; Dubolazov, A. V.; Mun, G. A. In *Hydrogen-Bonded Interpolymer Complexes: Formation, Structure and Applications*; Khutoryanskiy, V., Staikos, G., Eds.; World Scientific: Singapore, 2009.

(39) Kirsh, Y.; Soos, T.; Karaputadze, T. Chainlength effects on interactions of polyvinylpyrrolidone with low and high molecular compounds. *Eur. Polym. J.* **1979**, *15*, 223−228.

(40) Sorensen, C. M. Light Scattering by Fractal Aggregates: A Review. *Aerosol Sci. Technol.* **2001**, *35*, 648−687.

(41) Cattoz, B.; de Vos, W. M.; Cosgrove, T.; Crossman, M.; Appavou, M.-S.; Prescott, S. W. Complexation of polymeric stabilisers

DOI: 10.1021/la503870b
Langmuir 2015, 31, 4151−4159

in solution and at the silica nanoparticle interface. *Colloids Surf., A* **2014**, *449*, 57−64.
(42) Havlin, S.; Ben-Avraham, D. Fractal dimensionality of polymer chains. *J. Phys. A: Math. Gen.* **1982**, *15*, No. L311.
(43) Smith, W. E.; Zukoski, C. F. Hard Structured Particles: Suspension Synthesis, Characterization, and Compressibility. *Langmuir* **2004**, *20*, 11191−11200.
(44) Cattoz, B.; Cosgrove, T.; Crossman, M.; Prescott, S. W. Time-dependent depletion flocculation of silica nanoparticles. Manuscript in preparation.
(45) Nelson, A.; Jack, K. S.; Cosgrove, T.; Kozak, D. NMR Solvent Relaxation in Studies of Multicomponent Polymer Adsorption. *Langmuir* **2002**, *18*, 2750−2755.
(46) Flood, C.; Cosgrove, T.; Qiu, D.; Espidel, Y.; Howell, I.; Revell, P. Influence of a Surfactant and Electrolytes on Adsorbed Polymer Layers. *Langmuir* **2007**, *23*, 2408−2413 (PMID: 17309202).
(47) Hyodo, K.; Kobayashi, N.; Kagami, Y. The ion selective adsorption of polystyrenesulfonate onto a polyaniline surface. *Electrochim. Acta* **1991**, *36*, 799−802.
(48) Kang, Y.; Lee, M.-H.; Rhee, S. B. Electrochemical properties of polyaniline doped with poly(styrenesulfonic acid). *Synth. Met.* **1992**, *52*, 319−328.
(49) Bartlett, P. N.; Wang, J. H. Electroactivity, stability and application in an enzyme switch at pH 7 of poly(aniline)-poly-(styrenesulfonate) composite films. *J. Chem. Soc., Faraday Trans.* **1996**, *92*, 4137−4143.
(50) Frank, H. P.; Barkin, S.; Eirich, F. R. The Interaction of Polyvinylpyrrolidone with Some Azo Dyes. *J. Phys. Chem.* **1957**, *61*, 1375−1380.
(51) Molyneux, P.; Frank, H. P. The Interaction of Polyvinylpyrrolidone with Aromatic Compounds in Aqueous Solution. Part I. Thermodynamics of the Binding Equilibria and Interaction Forces. *J. Am. Chem. Soc.* **1961**, *83*, 3169−3174.
(52) Maruthamuthu, M.; Subramanian, E. Binding of benzopurpurin 4B to poly(N-vinyl-2-pyrrolidone): A spectral study on the mechanism of dye binding. *Colloid Polym. Sci.* **1990**, *268*, 256−263.

DOI: 10.1021/la503870b
Langmuir 2015, 31, 4151−4159